Editors' Suggestion | Featured in Physics

Schramm-Loewner Evolution in 2D Rigidity Percolation

Nina Javerzat*
SISSA and INFN Sezione di Trieste, via Bonomea 265, 34136, Trieste, Italy

(Received 15 February 2023; revised 25 August 2023; accepted 11 October 2023; published 2 January 2024)

Amorphous solids may resist external deformation such as shear or compression, while they do not present any long-range translational order or symmetry at the microscopic scale. Yet, it was recently discovered that, when they become rigid, such materials acquire a high degree of symmetry hidden in the disorder fluctuations: their microstructure becomes statistically conformally invariant. In this Letter, we exploit this finding to characterize the universality class of central-force rigidity percolation (RP), using Schramm-Loewner evolution (SLE) theory. We provide numerical evidence that the interfaces of the mechanically stable structures (rigid clusters), at the rigidification transition, are consistently described by SLE_κ, showing that this powerful framework can be applied to a mechanical percolation transition. Using well-known relations between different SLE observables and the universal diffusion constant κ, we obtain the estimation $\kappa \sim 2.9$ for central-force RP. This value is consistent, through relations coming from conformal field theory, with previously measured values for the clusters' fractal dimension D_f and correlation length exponent ν, providing new, nontrivial relations between critical exponents for RP. These findings open the way to a fine understanding of the microstructure in other important classes of rigidity and jamming transitions.

DOI: 10.1103/PhysRevLett.132.018201

Introduction.—Predicting the mechanical behavior of amorphous media, which have no long-range structural order, remains a challenge. Significant progress has been made in the last years to unify the description of disordered solids [1–3] like grain packings [4] or gels [5]. A lot remains to be understood though: indeed, very diverse materials from molecular glasses [6] and gels [7,8] to fibers [9–11] and living tissues [12–14] undergo a sudden transition between a fluid and a rigid state as an external parameter—e.g., the volume fraction of constituents—is varied. Such ability proves crucial, for instance, in biological processes like embryogenesis [12]. However, a quantitative understanding of the behavior of materials near rigidity transitions remains generally elusive. Can we find a unified description of rigidity transitions, predicting both the structural and mechanical properties of amorphous media at and close to their solidification point?

Rigidity percolation (RP) [15] plays a key role in this context, as a simple framework to model the emergence of mechanical stability in a disordered network: as the density of microscopic components is increased, they form structures, rigid under deformation, which eventually percolate the whole system, ensuring resistance to macroscopic constraints. The sudden change of mechanical state—from fluid to rigid—gets recast in the well-known language of percolation theory and controlled by the percolation order parameter, the probability that a network component belongs to the percolating rigid cluster. RP thus represents a general framework to model the solidification of amorphous media and has been successfully applied to understand the mechanical behavior of the materials listed above [6–14]. A considerable amount of work has been devoted to the onset of rigidity [7,9,10,16–29] corresponding in many cases to second-order transitions defining new universality classes. Their characterization remains, however, limited to the numerical measurement of the main critical exponents, e.g., ν and β controlling, respectively, the behavior of the correlation length and the order parameter at the transition.

RP is notably found to be distinct from connectivity percolation (CP) [19,28], which is simply defined by the emergence of a (nonrigid) percolating cluster and features a rich and well-studied critical behavior, with clusters becoming random fractals [30]. RP adds the *mechanical* dimension to the problem, making it intrinsically nonlocal, where the removal of a bond may destroy rigidity over a large region [19,22]. RP transitions remain, therefore, much less understood: the computation of the critical exponents, the possible connections with CP, and the possible unification of different RP universality classes are long-standing questions [16–18,22,23,28,29] still not fully resolved to date.

Recently, deep connections between CP and RP were uncovered. Liu *et al.* [28] studied minimal rigidity percolation (MRP), where the number of network's degrees of freedom matches exactly the number of constraints, and argued that it falls in the CP universality class. Even more recently [29], it was found, based on a numerical study of a particular set of observables, that central-force RP clusters are conformally invariant at the critical point. This opens the possibility to describe RP in the framework of

conformal field theory (CFT), in which scaling limits of observables are expressed as appropriate correlation functions [31]. Conformal invariance—the invariance of the statistical properties under local rescalings of the system—appears in many critical phenomena [32,33], but its emergence in RP is quite remarkable given the high nonlocality of the problem. Conformal symmetry has been used with great success to predict the universal properties of critical points [34–37] and notably allowed to determine exactly the critical exponents and other universal quantities in percolation [38–43]. For rigidity transitions too, exploiting conformal invariance can give access to the fine universal properties of the medium's microstructure. In addition to achieving a more complete characterization of the RP universality classes and their potential interconnections, this is also especially important regarding the prediction of the mechanical aspects of rigidity transitions. Indeed, the interplay between microstructure and elastic behavior at and near criticality has been recently highlighted in particulate materials [8]; although not systematically understood [9], it reveals that characterizing the microstructure near the transition—where structural heterogeneities develop at all length scales—is crucial to understand the mechanical response.

In this Letter, we investigate the RP universality class using Schramm-Loewner evolution (SLE) theory, a powerful framework to exploit conformal symmetry, which proved notably extremely successful to understand connectivity percolation [44]. We focus for simplicity on the case of purely central forces and consider the interfaces separating rigid clusters from floppy regions at criticality, known as the complete perimeters or hulls [30] of rigid percolating clusters (see inset of Fig. 3). In CP [45,46], as well as in diverse critical phenomena [47–54], the scaling limits of random interfaces are very interesting objects, as their probability measure possesses two remarkable properties, conformal invariance and a domain Markov property, which together yield powerful results about the universal class through the theory of SLE (see, e.g., [44,55,56] for introductions to the topic). The basic idea of SLE [45] is that a curve γ_t in a planar domain, parametrized by the time t can be equivalently encoded in a real function (the driving) ξ_t through a series of conformal maps g_t, such that the tip of the growing curve is $\gamma_t = g_t^{-1}(\xi_t)$. For a conformally invariant curve $\xi_t = \sqrt{\kappa}B_t$, with B_t a standard Brownian motion and κ a universal parameter known as the diffusion constant [45]. As a consequence of such remarkable equivalence, the scaling limit of the curve is determined by the value of κ only and many observables can be predicted exactly. This provides a classification of physically relevant random curves according to their value of κ [47,48,57–65]. The central charge c of the corresponding CFT is related to κ [66],

$$c = \frac{(8-3\kappa)(\kappa-6)}{2\kappa}. \tag{1}$$

c encodes how conformal symmetry manifests itself in the system and gives, e.g., the change in free energy when conformally transforming the system's geometry [67–69]. Its value is needed to compute physical observables and represents, therefore, crucial information about the universality class.

As we will argue, interfaces in RP are numerically consistent with SLE. In addition to giving access to more universal observables, this finding reveals the existence of a nontrivial algebraic structure in the underlying CFT through the existence of a so-called degenerate field [44,66]. This places the CFT of rigidity percolation in a more restricted class of field theories, to which connectivity percolation also belongs, and allows one to express RP critical exponents solely in terms of κ.

Model and methods.—We study central-force rigidity percolation on the site-diluted model with local correlations introduced in [7]: we populate randomly the sites of a triangular lattice of L_1 columns and L_2 rows with probability $p(\text{site}) = (1-\tilde{c})^{6-N_n(\text{site})}$, where N_n is the number of occupied nearest neighbors of that site. The short-range correlations introduced by taking $\tilde{c} > 0$ decrease the rigidity percolation threshold [7], allowing one to generate critical configurations of lower density, hence reducing the computation time, without affecting the long-range behavior so that universal quantities keep the same values as in the uncorrelated case [7,29]. We take $\tilde{c} = 0.3$, corresponding to a rigidity threshold $p_c \sim 0.657$ [7]. Rigid clusters are identified by the so-called pebble game [19] which, by efficient constraint counting, allows one to test the mutual rigidity of the bonds connecting occupied sites. We select the configurations where at least one rigid cluster percolates from bottom to top and construct, for each percolating cluster, its complete perimeter defined on the dual (hexagonal) lattice, as shown in the inset of Fig. 3; the hull of the rigid cluster (in blue) is highlighted as a dark line.

We stress that such unidirectionally percolating clusters have the same fractal structure as the cross-percolating ones, which ensure mechanical stability under global deformation. To study the random geometry of RP it is therefore sufficient to restrict to the former type of clusters, which are most adapted to the SLE analysis as detailed below.

We use the strip geometry, namely a large enough aspect ratio $L_1/L_2 = 4$, with periodic horizontal boundary conditions and open vertical boundary conditions, and systems as large as $L_2 = 1024$; sample averages, denoted $\mathbb{E}[\cdots]$, are performed over $N \geq 40\,000$ curves. Curves start from a point on the lower boundary and grow until they hit the upper boundary, and we therefore choose the framework of dipolar SLE [70], consistent with such a setup. In that case, the conformal maps g_t satisfy the Loewner equation [70]

TABLE I. Values of κ obtained from the fractal dimension, winding angle, left-passage probability (LPP), and zipper algorithm, as described in the text.

κ_{fractal}	κ_{winding}	κ_{LPP}	κ_{driving}
2.84(8)	2.88(5)	2.91(1)	2.7(1)

$$\frac{dg_t(z)}{dt} = \frac{\pi/L_y}{\tanh\left[\frac{\pi}{2L_y}(g_t(z)-\xi_t)\right]}, \qquad g_0(z) = z, \tag{2}$$

where $L_y = L_2\sqrt{3}/2$ is the width of the strip.

In the following sections, we (i) establish that the complete perimeters of the spanning rigid clusters are SLE_κ by showing that the statistics of their driving functions is compatible with a Brownian motion and (ii) obtain independent numerical estimates of the value of the diffusivity κ from the measurement of universal properties of the curves: their fractal dimension, winding angle, and left-passage probability. The results are summarized in Table I.

Driving function.—To extract numerically the driving ξ_t of a given curve, the idea is to solve Eq. (2) for each short time interval δt on which ξ_t is approximated as constant, obtaining the slit map g_t (see, e.g., [44,71]). Then, for each lattice curve $\{z_0^0 = 0, z_1^0, \ldots, z_l^0\}$ of length l starting at the origin, we compute iteratively the Loewner times t_j and the driving function ξ_{t_j} by successive applications of g_{t_j}, such that $t_0 = 0$, $\xi_{t_0} = 0$, and at each step the sequence $\{z_j^{j-1}, \ldots, z_l^{j-1}\}$, $j \geq 1$ is mapped to the reduced sequence $\{z_{j+1}^j = g_{t_j}(z_{j+1}^{j-1}), \ldots, z_l^j = g_{t_j}(z_l^{j-1})\}$. For dipolar SLE, the g_{t_j} are given by [48]

$$g_{t_j}(z) = \xi_{t_j} + \frac{2L_y}{\pi}\cosh^{-1}\left[\frac{\cosh\left[\frac{\pi}{2L_y}(z-\xi_{t_j})\right]}{\cos\Delta_j}\right], \tag{3}$$

where $\xi_{t_j} = \text{Re}(z_j^{j-1})$, $t_j = t_{j-1} - 2(L_y/\pi)^2\log(\cos\Delta_j)$, $\Delta_j = (\pi/2L_y)\text{Im}(z_j^{j-1})$, and we compute the complex inverse hyperbolic cosine as $\cosh^{-1}z = \log\left[z + i\sqrt{-z^2+1}\right]$. Each curve of length l is unzipped in this way for $l/2$ steps and yields an instance of the driving function ξ_t at sample-dependent, nonequally spaced Loewner times $t_0, \ldots, t_{l/2}$. We linearly interpolate each instance of the driving function to have all instances defined for a same, equally spaced time sequence.

Loewner's equation (2) holds for generic curves, and to claim that the rigid perimeters are indeed SLEs, we must ensure that the extracted driving function is a Brownian motion. The insets of Fig. 1 show the distributions of ξ_t at different times and the corresponding quantile-quantile plots, both consistent with Gaussian distributions. However, as studied by Kennedy [71], Gaussianity at fixed times

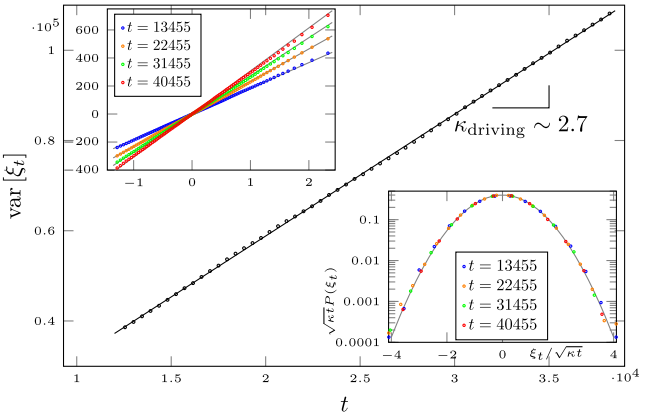

FIG. 1. Variance of the driving function ξ_t as a function of time. Bottom right inset: rescaled probability density function of ξ_t at four different times; in gray is the Gaussian distribution. Top left inset: quantile-quantile plots of ξ_t versus $\mathcal{N}(0,1)$ at four different times. Gray lines have slopes $\sqrt{\kappa_{\text{driving}}t}$.

alone is not an accurate test as it is passed by non-SLE processes as well, and one must test also the independence of the driving function's increments. Following [71] we pick n equally spaced times $0 < t_1 < \cdots < t_n$ and define the n increments $X_j \equiv \xi_{t_j+\delta} - \xi_{t_j}$. We set $\delta = 5$, but choosing a different value does not affect our conclusions as long as $\delta \ll \tau \equiv t_{j+1} - t_j$ (see also [48,63,65] where the correlation between two such consecutive increments is seen to decay for $\tau \gg \delta = 1$). The joint distribution of $(X_1, \ldots, X_n)$ is tested by defining $m = 2^n$ cells, each corresponding to the possible sign sequence of $(X_1, \ldots, X_n)$, counting the number O_j of samples falling in each cell and comparing with the expected value, $E_j = N/2^n$ for independent and Gaussian distributed variables. To this end, one defines

$$\chi^2 = \sum_{j=1}^{m}\frac{(O_j - E_j)^2}{E_j} \tag{4}$$

and computes the associated p value. Taking increasing numbers n of increments, with $t_k \in [9.10^3, 29.10^3]$, we find $p_{n=5} = 0.95$, $p_{n=7} = 0.78$, and $p_{n=9} = 0.81$.

These p values are not small, indicating that one cannot reject the hypothesis that ξ_t is a Brownian motion. This leads to our first main result, that the statistics of the hulls of rigid RP clusters are consistent with SLE.

The driving function straightforwardly gives a first estimate of the diffusion constant, since by definition $\text{var}[\xi_t] = \kappa t$. The main plot of Fig. 1 shows the variance of ξ as a function of time, and a fit gives the value κ_{driving} reported in Table I.

It was observed, however, that the estimation of κ from the driving function comes with non-negligible error [63]. In the next sections, we therefore use standard results on SLE to obtain independent and more accurate estimations of κ from more directly measurable quantities.

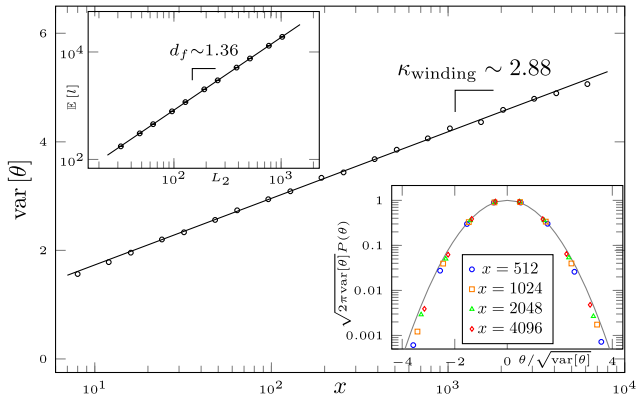

FIG. 2. Variance of the winding angle θ as function of the distance x along the curve. Top left inset: mean length $\mathbb{E}[l]$ of the curves as function of the system height L_2. Bottom right inset: rescaled probability density function of the winding angle at different distances x; in gray is the Gaussian distribution.

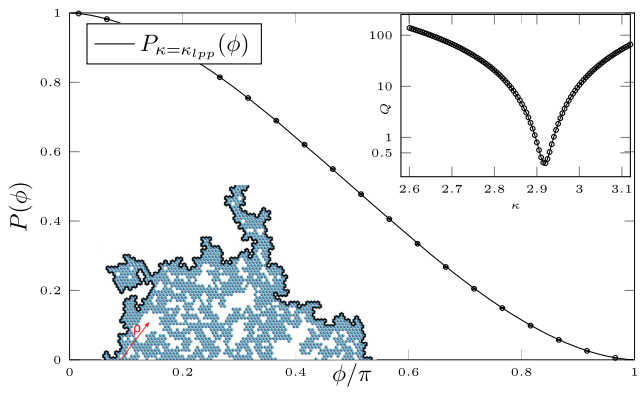

FIG. 3. Left-passage probability of spanning perimeters and the prediction (6) for $\kappa = \kappa_{\text{LPP}}$. Top right inset: weighted mean-square deviation Q given by (7). Bottom left inset: example of a rigid cluster (blue) and its left and right hulls (black thick lines). The right hull passes to the left of the point located at $z = \rho e^{i\phi}$ from its origin, marked as a red vector.

Fractal dimension.—For a spanning curve of lattice length l the fractal dimension can be defined as $l \sim L_2^{d_f}$. For SLEs, d_f is related to the diffusivity by $d_f = 1 + \kappa/8$ [72]. The inset of Fig. 2 displays the average length $\mathbb{E}[l]$ of the spanning perimeters versus the lattice system height $L_2 \in [32, 1024]$; fitting gives $d_f = 1.355 \pm 0.01$, corresponding to the value κ_{fractal} given in Table I.

Winding angle.—How tortuous an SLE is can be exactly predicted: the winding angle measured between two typical points along the curve is Gaussian distributed, with a variance that grows logarithmically with the distance between the points [45,57,59,73]. On the lattice we define $\theta_j = \sum_{i=1}^{j} \alpha_i$, the sum of the local turns α_i that the curve takes at each step of its growth. In the scaling limit, we expect that, at distance x along the curve from the starting point, the variance of θ is [59,60]

$$\text{var}[\theta(x)] = a + \frac{2\kappa}{8+\kappa} \log x. \tag{5}$$

The inset of Fig. 2 shows the rescaled distribution of θ at different distances x, falling on the Gaussian distribution, while the main plot shows its variance as function of x. Fitting according to (5) we obtain the estimation κ_{winding} of Table I.

Left-passage probability.—A famous result on SLE is the probability of the curve passing to the left of a given point in the upper-half plane. With the curve starting at the origin, this probability for a point $z = \rho e^{i\phi}$ depends only on ϕ and reads [74]

$$P_\kappa(\phi) = \frac{1}{2} + \frac{\Gamma(\frac{4}{\kappa})}{\sqrt{\pi}\Gamma(\frac{8-\kappa}{2\kappa})} \cot(\phi) {}_2F_1\left[\frac{1}{2}, \frac{4}{\kappa}, \frac{3}{2}, -\cot^2(\phi)\right], \tag{6}$$

where ${}_2F_1$ is the ordinary hypergeometric function. This prediction is seen to hold as well for dipolar curves not too far from their starting point, i.e., $\rho \ll L_y$ [48,61]. We measure the left-passage probability $P(z)$ for a fixed set $\mathcal{S}$ of about 300 points in the semiannulus $(\rho, \phi) \in [L_y/16, L_y/4] \times (0, \pi)$. We estimate κ as the value minimizing the mean-square deviation $Q(\kappa)$ [62],

$$Q(\kappa) \equiv \frac{N-1}{|S|} \sum_{z \in S} \frac{\left[P(z) - P_\kappa[\phi(z)]\right]^2}{P(z)[1-P(z)]}. \tag{7}$$

Q is plotted in the inset of Fig. 3; minimizing the interpolating function, we find the estimate κ_{LPP} reported in Table I. The main plot of Fig. 3 shows the data points for $P(z)$ averaged over ρ for each value of ϕ, together with the prediction $P_{\kappa_{\text{LPP}}}$ of Eq. (6).

Critical exponents.—Interfaces in RP being SLEs have consequences on the structural properties. It implies the existence of a so-called degenerate field $\Phi_{2,1}$ of dimension $h_{2,1} = (6-\kappa)/(2\kappa)$ [44,66], whose correlation functions satisfy differential equations [34,35], leading, in particular, to relations involving the clusters' critical exponents [75,76]. We find that the previously measured RP fractal dimension $D_f = 1.86(2)$ [7,19] is indeed consistent with the prediction [77] $D_f(\kappa) = 1 + 3/(2\kappa) + \kappa/8 \sim 1.88$, where we used our value $\kappa_{\text{RP}} \sim 2.9$. Moreover, there is also good agreement between the value of the correlation length exponent $\nu = 1.21(6)$ [19] and the expression [77] $\nu(\kappa) = (2 - 2h_{2,1})^{-1} = \kappa/(3\kappa - 6) \sim 1.1$. These two expressions give, for generic $\kappa \geq 4$, the critical exponents of the Q-state Potts model geometric clusters [49,50,77].

Conclusion.—Using SLE theory, we first gave numerical evidence that the perimeters of spanning central-force RP clusters are SLE$_\kappa$ processes. We obtained independent estimates of the universal diffusion constant $\kappa_{\text{RP}} \sim 2.9$, which by (1) corresponds to a central charge $c_{\text{RP}} \sim 0.37$. These findings, along with the ones in [29], show that the

rigorous approaches of SLE and CFT can be applied to the study of random geometry in a *mechanical* percolation transition such as RP. Notably, SLE and CFT allow one, by exploiting symmetry constraints, to express critical exponents solely in terms of κ, finding good numerical agreement with the values measured by standard techniques [7,19]. Whether the value of κ_{RP} corresponds to some simple fraction, which would lead to exact predictions for the RP critical exponents, remains a tantalizing possibility.

At this stage, it seems important to understand better the connection between RP and CP. Simulations of site- or bond-diluted RP show that a typical RP cluster consists of overconstrained regions and isostatic (minimally rigid) dangling ends [19,20,22]. According to [28], clusters without overconstrained regions would fall in the CP universality class, so we expect that the latter drive the system to the distinct RP critical point. It would be useful, therefore, to tune the fraction of overconstrained regions (e.g., cutting redundant bonds [25]), to interpolate between RP and MRP (CP), and analyze these transitions using the methods of the present Letter. One could also check if rigid hulls in MRP are indeed equivalent to CP hulls: in that case, we expect correspondence with the percolation accessible perimeters [30] that are $\mathrm{SLE}_{8/3}$ [78,79].

More generally, our results open the way to applying the SLE analysis to other important classes of rigidity transitions besides central force, providing a new tool to analyze in detail the microstructure of disordered media at the onset of rigidity. A case particularly worth investigating is the frictional jamming transition [26,28], where rigid clusters can be identified. It would be very interesting to examine if conformal invariance remains unbroken and whether the critical exponents can be correctly predicted from SLE.

It is a pleasure to thank O. Abuzaid, F. Ares, M. Bouzid, X. Cao, G. Delfino, N. El-Kazwini, D. X. Horvath, Y. Ikhlef, J. Jacobsen, S. Ribault, R. Santachiara, and B. Walter for very valuable and stimulating discussions, as well as useful comments on the Letter. I acknowledge support from European Research Council (ERC) under consolidator Grant No. 771536 [NEMO].

*njaverza@sissa.it

[1] Silke Henkes and Bulbul Chakraborty, Statistical mechanics framework for static granular matter, Phys. Rev. E **79**, 061301 (2009).
[2] E. DeGiuli, Field theory for amorphous solids, Phys. Rev. Lett. **121**, 118001 (2018).
[3] Jishnu N. Nampoothiri, Yinqiao Wang, Kabir Ramola, Jie Zhang, Subhro Bhattacharjee, and Bulbul Chakraborty, Emergent elasticity in amorphous solids, Phys. Rev. Lett. **125**, 118002 (2020).
[4] Jishnu N. Nampoothiri, Michael D'Eon, Kabir Ramola, Bulbul Chakraborty, and Subhro Bhattacharjee, Tensor electromagnetism and emergent elasticity in jammed solids, Phys. Rev. E **106**, 065004 (2022).
[5] H. A. Vinutha, Fabiola Doraly Diaz Ruiz, Xiaoming Mao, Bulbul Chakraborty, and Emanuela Del Gado, Stress–stress correlations reveal force chains in gels, J. Chem. Phys. **158**, 114104 (2023).
[6] M. F. Thorpe, D. J. Jacobs, M. V. Chubynsky, and J. C. Phillips, Self-organization in network glasses, J. Non-Cryst. Solids **266–269**, 859 (2000).
[7] Shang Zhang, Leyou Zhang, Mehdi Bouzid, D. Zeb Rocklin, Emanuela Del Gado, and Xiaoming Mao, Correlated rigidity percolation and colloidal gels, Phys. Rev. Lett. **123**, 058001 (2019).
[8] Minaspi Bantawa, Bavand Keshavarz, Michela Geri, Mehdi Bouzid, Thibaut Divoux, Gareth H. McKinley, and Emanuela Del Gado, The hidden hierarchical nature of soft particulate gels, Nat. Phys. **19**, 1178 (2023).
[9] D. A. Head, F. C. MacKintosh, and A. J. Levine, Nonuniversality of elastic exponents in random bond-bending networks, Phys. Rev. E **68**, 025101(R) (2003).
[10] Chase P. Broedersz, Xiaoming Mao, Tom C. Lubensky, and Frederick C. MacKintosh, Criticality and isostaticity in fibre networks, Nat. Phys. **7**, 983 (2011).
[11] Bekele J. Gurmessa, Nicholas Bitten, Dan T. Nguyen, Omar A. Saleh, Jennifer L. Ross, Moumita Das, and Rae M. Robertson-Anderson, Triggered disassembly and reassembly of actin networks induces rigidity phase transitions, Soft Matter **15**, 1335 (2019).
[12] Nicoletta I. Petridou, Bernat Corominas-Murtra, Carl-Philipp Heisenberg, and Edouard Hannezo, Rigidity percolation uncovers a structural basis for embryonic tissue phase transitions, Cell **184**, 1914 (2021).
[13] Thomas Wyse Jackson, Jonathan Michel, Pancy Lwin, Lisa A. Fortier, Moumita Das, Lawrence J. Bonassar, and Itai Cohen, Structural origins of cartilage shear mechanics, Sci. Adv. **8**, eabk2805 (2022).
[14] Pierre-François Lenne and Vikas Trivedi, Sculpting tissues by phase transitions, Nat. Commun. **13**, 664 (2022).
[15] M. F. Thorpe, Continuous deformations in random networks, J. Non-Cryst. Solids **57**, 355 (1983).
[16] P. G. De Gennes, On a relation between percolation theory and the elasticity of gels, J. Phys. Lett. **37**, 1 (1976).
[17] Shechao Feng and Pabitra N. Sen, Percolation on elastic networks: New exponent and threshold, Phys. Rev. Lett. **52**, 216 (1984).
[18] Yacov Kantor and Itzhak Webman, Elastic properties of random percolating systems, Phys. Rev. Lett. **52**, 1891 (1984).
[19] D. J. Jacobs and M. F. Thorpe, Generic rigidity percolation: The pebble game, Phys. Rev. Lett. **75**, 4051 (1995).
[20] C. Moukarzel, P. M. Duxbury, and P. L. Leath, Infinite-cluster geometry in central-force networks, Phys. Rev. Lett. **78**, 1480 (1997).
[21] P. M. Duxbury, C. Moukarzel, and P. L. Leath, Duxbury, Moukarzel and Leath reply, Phys. Rev. Lett. **80**, 5452 (1998).
[22] C. Moukarzel and P. M. Duxbury, Comparison of rigidity and connectivity percolation in two dimensions, Phys. Rev. E **59**, 2614 (1999).

[23] Michael Plischke, Rigidity of disordered networks with bond-bending forces, Phys. Rev. E **76**, 021401 (2007).
[24] Leyou Zhang, D. Zeb Rocklin, Bryan Gin-ge Chen, and Xiaoming Mao, Rigidity percolation by next-nearest-neighbor bonds on generic and regular isostatic lattices, Phys. Rev. E **91**, 032124 (2015).
[25] Wouter G. Ellenbroek, Varda F. Hagh, Avishek Kumar, M. F. Thorpe, and Martin van Hecke, Rigidity loss in disordered systems: Three scenarios, Phys. Rev. Lett. **114**, 135501 (2015).
[26] Silke Henkes, David A. Quint, Yaouen Fily, and J. M. Schwarz, Rigid cluster decomposition reveals criticality in frictional jamming, Phys. Rev. Lett. **116**, 028301 (2016).
[27] Danilo B. Liarte, O. Stenull, Xiaoming Mao, and T. C. Lubensky, Elasticity of randomly diluted honeycomb and diamond lattices with bending forces, J. Phys. Condens. Matter **28**, 165402 (2016).
[28] Kuang Liu, S. Henkes, and J. M. Schwarz, Frictional rigidity percolation: A new universality class and its superuniversal connections through minimal rigidity proliferation, Phys. Rev. X **9**, 021006 (2019).
[29] Nina Javerzat and Mehdi Bouzid, Evidences of conformal invariance in 2D rigidity percolation, Phys. Rev. Lett. **130**, 268201 (2023).
[30] D. Stauffer and A. Aharony, *Introduction to Percolation Theory* (Oxford University Press, New York, 1971).
[31] John Cardy, Exact Methods in Low-dimensional Statistical Physics and Quantum Computing, *Lecture Notes of the Les Houches Summer School*, edited by Jesper Jacobsen, Stephane Ouvry, Vincent Pasquier, Didina Serban, and Leticia Cugliandolo (2008), Vol. 89.
[32] Alexander M. Polyakov, Conformal symmetry of critical fluctuations, JETP Lett. **12**, 381 (1970).
[33] P. Di Francesco, P. Mathieu, and D. Senechal, *Conformal Field Theory*, Graduate Texts in Contemporary Physics (Springer-Verlag, New York, 1997).
[34] A. A. Belavin, A. M. Polyakov, and A. B. Zamolodchikov, Infinite conformal symmetry of critical fluctuations in two dimensions, J. Stat. Phys. **34**, 763 (1984).
[35] A. A. Belavin, A. M. Polyakov, and A. B. Zamolodchikov, Infinite conformal symmetry in two-dimensional quantum field theory, Nucl. Phys. **B241**, 333 (1984).
[36] Daniel Friedan, Zongan Qiu, and Stephen Shenker, Conformal invariance, unitarity, and critical exponents in two dimensions, Phys. Rev. Lett. **52**, 1575 (1984).
[37] David Poland and David Simmons-Duffin, The conformal bootstrap, Nat. Phys. **12**, 535 (2016).
[38] H. Saleur and B. Duplantier, Exact determination of the percolation hull exponent in two dimensions, Phys. Rev. Lett. **58**, 2325 (1987).
[39] P. di Francesco, H. Saleur, and J. B. Zuber, Relations between the Coulomb gas picture and conformal invariance of two-dimensional critical models, J. Stat. Phys. **49**, 57 (1987).
[40] J. L. Cardy, Critical percolation in finite geometries, J. Phys. A **25**, L201 (1992).
[41] Gesualdo Delfino and Jacopo Viti, On three-point connectivity in two-dimensional percolation, J. Phys. A **44**, 032001 (2010).
[42] Marco Picco, Sylvain Ribault, and Raoul Santachiara, A conformal bootstrap approach to critical percolation in two dimensions, SciPost Phys. **1**, 009 (2016).
[43] Yifei He, Jesper Lykke Jacobsen, and Hubert Saleur, Geometrical four-point functions in the two-dimensional critical q-state Potts model: The interchiral conformal bootstrap, J. High Energy Phys. 12 (2020) 019.
[44] John Cardy, SLE for theoretical physicists, Ann. Phys. (Amsterdam) **318**, 81 (2005), special issue.
[45] Oded Schramm, Scaling limits of loop-erased random walks and uniform spanning trees, Isr. J. Math. **118**, 221 (2000).
[46] Federico Camia and Charles M. Newman, Critical percolation exploration path and SLE6: A proof of convergence, Probab. Theory Related Fields **139**, 473 (2007).
[47] C. Amoruso, A. K. Hartmann, M. B. Hastings, and M. A. Moore, Conformal invariance and stochastic Loewner evolution processes in two-dimensional Ising spin glasses, Phys. Rev. Lett. **97**, 267202 (2006).
[48] D. Bernard, P. Le Doussal, and A. A. Middleton, Possible description of domain walls in two-dimensional spin glasses by stochastic Loewner evolutions, Phys. Rev. B **76**, 020403 (R) (2007).
[49] Stanislav Smirnov, Towards conformal invariance of 2D lattice models (2006), pp. 1421–1451, https://archive-ouverte.unige.ch/unige:12063.
[50] Adam Gamsa and John Cardy, Schramm–Loewner evolution in the three-state Potts model–A numerical study, J. Stat. Mech. (2007) P08020.
[51] Raoul Santachiara, SLE in self-dual critical $Z(N)$ spin systems: CFT predictions, Nucl. Phys. **B793**, 396 (2008).
[52] Jesper L. Jacobsen, Pierre Le Doussal, Marco Picco, Raoul Santachiara, and Kay Jörg Wiese, Critical interfaces in the random-bond Potts model, Phys. Rev. Lett. **102**, 070601 (2009).
[53] Steffen Rohde and Oded Schramm, *Basic Properties of SLE* (Springer, New York, 2011), pp. 989–1030.
[54] M. Caselle, S. Lottini, and M. A. Rajabpour, Critical domain walls in the Ashkin–Teller model, J. Stat. Mech. (2011) P02039.
[55] Wouter Kager, Bernard Nienhuis, and Leo P. Kadanoff, Exact solutions for Loewner evolutions, J. Stat. Phys. **115**, 805 (2004).
[56] Michel Bauer and Denis Bernard, 2D growth processes: SLE and Loewner chains, Phys. Rep. **432**, 115 (2006).
[57] Benjamin Wieland and David B. Wilson, Winding angle variance of Fortuin-Kasteleyn contours, Phys. Rev. E **68**, 056101 (2003).
[58] Denis Bernard, Guido Boffetta, Antonio Celani, and Gregory Falkovich, Conformal invariance in two-dimensional turbulence, Nat. Phys. **2**, 124 (2006).
[59] G. Boffetta, A. Celani, D. Dezzani, and A. Seminara, How winding is the coast of Britain? Conformal invariance of rocky shorelines, Geophys. Res. Lett. **35** (2008).
[60] A. A. Saberi and S. Rouhani, Scaling of clusters and winding-angle statistics of isoheight lines in two-dimensional Kardar-Parisi-Zhang surfaces, Phys. Rev. E **79**, 036102 (2009).
[61] A. A. Saberi, H. Dashti-Naserabadi, and S. Rouhani, Classification of $(2+1)$-dimensional growing surfaces using

Schramm-Loewner evolution, Phys. Rev. E **82**, 020101(R) (2010).
[62] E. Daryaei, N. A. M. Araújo, K. J. Schrenk, S. Rouhani, and H. J. Herrmann, Watersheds are Schramm-Loewner evolution curves, Phys. Rev. Lett. **109**, 218701 (2012).
[63] N. Posé, K. J. Schrenk, N. A. M. Araújo, and H. J. Herrmann, Shortest path and Schramm-Loewner evolution, Sci. Rep. **4**, 5495 (2014).
[64] I. Giordanelli, N. Posé, M. Mendoza, and H. J. Herrmann, Conformal invariance of graphene sheets, Sci. Rep. **6**, 22949 (2016).
[65] C. P. de Castro, M. Luković, G. Pompanin, R. F. S. Andrade, and H. J. Herrmann, Schramm-Loewner evolution and perimeter of percolation clusters of correlated random landscapes, Sci. Rep. **8**, 5286 (2018).
[66] Michel Bauer and Denis Bernard, SLE_κ growth processes and conformal field theories, Phys. Lett. B **543**, 135 (2002).
[67] H. W. J. Blöte, John L. Cardy, and M. P. Nightingale, Conformal invariance, the central charge, and universal finite-size amplitudes at criticality, Phys. Rev. Lett. **56**, 742 (1986).
[68] Ian Affleck, Universal term in the free energy at a critical point and the conformal anomaly, Phys. Rev. Lett. **56**, 746 (1986).
[69] John L. Cardy, *Scaling and Renormalization in Statistical Physics* (Cambridge University Press, Cambridge, 1996).
[70] M. Bauer, D. Bernard, and J. Houdayer, Dipolar stochastic Loewner evolutions, J. Stat. Mech. (2005) P03001.
[71] Tom Kennedy, Computing the Loewner driving process of random curves in the half plane, J. Stat. Phys. **131**, 803 (2008).
[72] Vincent Beffara, The dimension of the SLE curves, Ann. Probab. **36**, 1421 (2008).
[73] Bertrand Duplantier and Hubert Saleur, Winding-angle distributions of two-dimensional self-avoiding walks from conformal invariance, Phys. Rev. Lett. **60**, 2343 (1988).
[74] Oded Schramm, A percolation formula, Electron. Commun. Probab. **6**, 115 (2001).
[75] John Cardy, Calogero–Sutherland model and bulk-boundary correlations in conformal field theory, Phys. Lett. B **582**, 121 (2004).
[76] B. Doyon and J. Cardy, Calogero–Sutherland eigenfunctions with mixed boundary conditions and conformal field theory correlators, J. Phys. A **40**, 2509 (2007).
[77] Wolfhard Janke and Adriaan M. J. Schakel, Geometrical vs Fortuin–Kasteleyn clusters in the two-dimensional q-state Potts model, Nucl. Phys. **B700**, 385 (2004).
[78] Bertrand Duplantier, Conformally invariant fractals and potential theory, Phys. Rev. Lett. **84**, 1363 (2000).
[79] Vincent Beffara, Hausdorff dimensions for SLE6, Ann. Probab. **32**, 2606 (2004).